Materials Today Sustainability 19 (2022) 100190

Contents lists available at ScienceDirect

Materials Today Sustainability

journal homepage: https://www.journals.elsevier.com/materials-today-sustainability

Effective $^{137}Cs^{+}$ and $^{90}Sr^{2+}$ immobilisation from groundwater by inorganic polymer resin Clevasol® embedded within a macroporous cryogel host matrix

J.D. Chaplin [a, *, c], D. Berillo [b, e], J.M. Purkis [a], M.L. Byrne [a, d], A.D.C.C.M. Tribolet [a], P.E. Warwick [a], A.B. Cundy [a]

[a] School of Ocean and Earth Science, University of Southampton, National Oceanography Centre, Southampton, SO14 3ZH, UK
[b] School of Pharmacy and Biomolecular Sciences, University of Brighton, Brighton, BN2 4GJ, UK

ARTICLE INFO

Article history:
Received 20 April 2022
Received in revised form
17 June 2022
Accepted 30 June 2022
Available online 6 July 2022

Keywords:
Strontium
Cesium/cesium
Remediation
Sellafield
Radionuclides
Environmental radioactivity

ABSTRACT

The conservative fission products ^{137}Cs and ^{90}Sr are of concern when present in groundwater, as they present a radiological hazard to organisms and can be transported long distances from their source. To provide an interceptive permeable reactive barrier (PRB) solution which accommodates the throughflow of groundwater whilst removing $^{137}Cs^{+}$ and $^{90}Sr^{2+}$, we report the synthesis of a novel composite cryogel which performs as a permeable hierarchical sorbent. This material incorporates the ion-exchanger Clevasol® into a PVA-based cryogel host matrix with interconnected macropores, producing a composite cryogel (Clevasol®-PVACC). Clevasol®-PVACC enables the *in-situ* deployment of an ion-exchanger with rapid uptake kinetics for $^{137}Cs^{+}$ and $^{90}Sr^{2+}$, inside of a robust and permeable scaffold with green chemistry. Clevasol®-PVACC has a facile, one-pot and scalable synthesis, and can possibly also be used at other stages of the nuclear fuel cycle, such as radioactive liquor treatment. Critically, the incorporated Clevasol® resin is vitrifiable, which is optimal for long-term storage and geological disposal if high activities are adhered onto the resin. The effective partition coefficients (k_d) and effective Langmuir uptake capacities (q_{max}) of the Clevasol® resin in Sellafield groundwater simulant are respectively 10^5 mL/g and 298 mg/g for Cs^{+}, and $>10^4$ mL/g and 128 mg/g for Sr^{2+}.

1. Introduction

1.1. ^{137}Cs and ^{90}Sr discharges

Fission products (FPs) are radionuclides resulting from splitting of fissile nuclei in nuclear reactors and weapons. Following decades of authorised discharges from nuclear facilities (*e.g.* Sellafield, UK; Hanford, USA; Majak, former USSR), nuclear accidents (*e.g.* Fukushima-Daïchi, Japan; Chernobyl, former USSR) and stratospheric fallout from atomic testing, FPs are widespread in the environment and present an ongoing and sometimes severe risk to health when present in elevated concentrations. Two FPs of particular concern are ^{137}Cs and ^{90}Sr; both are high-energy β^{-}-emitters which persist in the environment in significant quantities due to their high ^{235}U-fission yields and ~30-year half-lives.

Cs and Sr occur in the aqueous phase as hydrated cations (Cs^{+} and Sr^{2+}), which are typically inert to pH and speciation changes within environmental physicochemical parameters. They are present as the free ion in environmental conditions and are highly mobile in the aqueous phase. Water-transport pathways such as groundwater can therefore transport $^{137}Cs^{+}$ and $^{90}Sr^{2+}$ to the oceans, where both FPs can bioaccumulate in seafood and can therefore transfer to the human food chain. The presence of $^{137}Cs^{+}$ and $^{90}Sr^{2+}$ in groundwater is therefore of particular concern.

Removing $^{137}Cs^{+}$ and $^{90}Sr^{2+}$ from the environment helps to limit the long-term radiation exposure to biota; developing novel sorbent materials for these pollutants therefore contributes to the long-term sustainability of otherwise-contaminated environments.

* Corresponding author.
E-mail address: joshua.chaplin@chuv.ch (J.D. Chaplin).
[c] Present Addresses. Institute of Radiation Physics, Lausanne University Hospital, 1 Rue du Grand-Pré, 1007 Lausanne, Vaud, Switzerland.
[d] Present Addresses. Dounreay Site Restoration Ltd, Dounreay, Thurso, Caithness, KW14 7JJ, United Kingdom.
[e] Present Addresses. Department of Pharmaceutical and Toxicological chemistry, Pharmacognosy and botany, School of Pharmacy, Asfendiyarov Kazakh National Medical University, Almaty, Kazakhstan.

https://doi.org/10.1016/j.mtsust.2022.100190

Abbreviations

PRB	Permeable reactive barrier
PVACC	Poly(vinyl alcohol)-based cryogel-composite
FP	Fission Product
GA	Glutaraldehyde
CHI	Chitosan
SSA	Specific Surface Area(s)
SEM	Scanning Electron Microscopy
SGS	Sellafield Groundwater Simulant
HPGe	High Purity Germanium
ICP-OES	Inductively Coupled Plasma Optical Emission Spectrometry
ICP-QQQ	Inductively Coupled Plasma Triple Quadrupole Mass Spectrometry
ICP-MS	Inductively Coupled Plasma Mass Spectrometry

At Sellafield alone, there is estimated to be up to 2,000,000 m^3 of contaminated land [1], in which ^{90}Sr has been identified in the groundwater table [2]. At the Hanford site in the USA, 3,750,000 L of liquid waste containing FPs has been estimated to have leaked from corrodible storage tanks [3], and uncontrolled releases of Sr and Cs into the Pacific from the Fukushima-Daïchi plant through groundwater and freshwater continued for many years after the catastrophe [4–8]. With the rapid projected growth of nuclear power (by up to 56% by 2030 compared to 2015 levels) [9], more nuclear waste is produced, meaning more ^{137}Cs and ^{90}Sr will invariably enter the environment. Materials that can rapidly and effectively remediate these highly hazardous and radiotoxic pollutants are therefore a crucial requirement.

1.2. Sorbents for Cs and Sr

At present, a range of sorbents have been reported which can effectively immobilise $^{137}Cs^{+}$ and $^{90}Sr^{2+}$ from groundwater in natural conditions, through extractant processes such as cation-exchange [10,11]. These include, but are not limited to, natural clays [12,13]; natural and synthetic zeolites [14,15] (particularly clinoptilolite, which has been deployed practically in permeable reactive barrier (PRB) systems [16,17] and in effluent flocculation treatment [18]); activated organic matter [19–22]; cation-exchange resins [15,23,24]; ferrocyanides/hexacyanoferrates [25,26], and ammonium molybdophosphate ($[NH_4]_3$ $[PMo_{12}O_{40}]$) [27–30]. Novel sorbents with improved characteristics for practical implementation (including capacity and uptake kinetics for their target contaminants, cost, and scalability of manufacture etc.) are continually developed, to produce more effective and efficient remediation solutions [31]. The selectivity of a sorbent for its target contaminant(s) in the presence of spectator ions is a critical trait, particularly for short-to-medium lived radionuclides whose mass concentrations in the aqueous phase are very small. Having a high selectivity for its target contaminant(s) ensures that a sorbent remains effective in solutions of higher ionic strength (groundwater, seawater, *etc.*). Environmental stability and suitability for reuse, storage or geological disposal are also important considerations for resource conservation, handling, and waste management. We direct the reader to some recent review articles for a comparison of the performance parameters, including for example the partition coefficient (k_d) and uptake capacity (q_{max}), of a range of adsorbents employed for Cs^{+} sorption [32–35] and Sr^{2+} sorption [35,36], In this work, we report the first practical implementation of the recently developed inorganic polymer resin Clevasol® to capture Cs^{+} and Sr^{2+} from simulated Sellafield site groundwater.

1.3. Host matrices for sorbents

To provide a practical solution to deploy fine-grained and potentially mobile sorbent particles *in-situ* in the environment (such as for example in the development of PRBs), various matrices have been reported which provide a permeable host for the particles [37]. These include, but are not limited to, SiO_2 [29,30], starch [38], organic biocomposites [39], polyacrylamide [40,41] and chitosan [42]. Embedding sorbent particles in materials with interconnected pores such as these allows for the throughflow of contaminated solutions. In this work, we use cryogels as a permeable host matrix for Clevasol® particles. Cryogels offer many advantages over alternative materials; for example, their mode of configuration is flexible (*e.g.* they can be manufactured with different polymers including PVA [43] and chitosan [44–46], and in varying shapes and sizes [47]); their manufacture is simple, low-cost and scalable [47], and they have a high resistance to hydrostatic pressure with negligible flow resistance [47,48]. Cryogels with embedded adsorbents have also been used to successfully treat solutions contaminated with a variety of inorganic wastes (*e.g.* As [47], Hg [49]) and organic wastes (*e.g.* 4-nitrophenol [50], pesticides atrazine and malathion [51]). However, the use of cryogels as supports for PRB materials for radionuclide sorption has yet to be explored.

1.4. Scope of this work

Herein, we report the synthesis, characterisation and implementation of a composite material which incorporates particles of the Clevasol® resin into a poly (vinyl alcohol) (PVA)-based cryogel host matrix. We refer to this material herein as Clevasol®-PVACC (Clevasol®-PVA-cryogel-composite) and perform a range of testing to assess its suitability for the intended purpose of *in-situ* PRB deployment.

2. Material and methods

2.1. Material synthesis

All reagents used were of analytical grade. To manufacture Clevasol®-PVACC, we prepared 10 g of a mixture constituting 10 wt% Clevasol® particles (200 ± 100 μm diameter), 5 wt% PVA (Sigma-Aldrich), 0.25 wt% glutaraldehyde (GA, 50% aqueous, Fisher Scientific) and 84.75 wt% Milli-Q H_2O. The pH was adjusted to ≤2 with dropwise addition of 2 M HCl during magnetic stirring to promote homogenous particle distribution. This mixture was dispersed in an ultrasonic bath for 10 s then immediately transferred into pre-cooled glass tubes in a cryostat at −12 °C. This process freezes the H_2O, forming porogenic ice crystals in the polymer structure [52–54]. The mixture froze within seconds, avoiding significant particle settling. Tubes were left in the cryostat for 48 h before thawing, allowing the formation of a highly cross-linked polymer with a continuous system of interconnected macropores (Fig. SI III of the Supporting Information). Additionally, two batches of blank cryogel were manufactured without any Clevasol® particles: a) PVA and GA-based (as above), and b) chitosan (CHI) and GA (1 wt% CHI, 0.25 wt% GA). This allowed PVA and CHI to be compared as the cryogel polymer, in regard to the effects on the specific surface area (SSA) and structural integrity of the cryogels. All cryogels were stored saturated in Milli-Q H_2O and refrigerated at 4 °C.

2.2. Sellafield groundwater simulant (SGS)

SGS was prepared as per Table SI II in the Supporting Information and used in all experiments at pH 7.1 and room temperature (25 °C).

2.3. SEM

1 mm-thick slices of the cryogels and composite cryogels were cut using a blade and washed with Milli-Q H_2O. The cryogel slices were fixed in 5% GA solution overnight and washed again with Milli-Q H_2O. Wet cryogels were frozen at −80 °C for 3 h before being placed into a Christ ALPHA 2–4 freeze-dryer for 24 h. For SEM study, the freeze-dried samples were coated with a layer of Pt using a Quorum (Q150TES) coater and scanned using a Zeiss Sigma field emission gun SEM (Zeiss NTS). A Carl Zeiss Leo 1450VP SEM with Oxford Instruments Energy Dispersive Spectrometer was also used to analyse vacuum-filtered non-bound Clevasol® particles, before and after 48 h of exposure to 1000 ppm Sr or Cs in Milli-Q H_2O.

2.4. N_2 adsorption-desorption

SSA data were produced using a Quantachrome ASiQwinGAS instrument, following outgassing of samples at 200 °C for 3 h. N_2-adsorption and desorption tests were performed at relative pressures and temperature of 77.4 K. SSA was estimated applying the BET method and the pore size distributions of the materials were estimated using both BJH and DFT methods [52].

2.5. Mechanical properties

Stress-strain regimes and Young's moduli were determined with a TA-XT2 instrument (Stable Micro Systems, Surrey, UK), using a 0.05 mm/s velocity 50 mm diameter plunger at up to 35–40% sample compression. Young's modulus (E_Y, Pa) was determined from the gradient of the linear region of the stress-strain regime that the materials demonstrated at <2.5% compression, per Eq. (1) [44]:

$$E_Y = \frac{(Fh)}{(A\Delta h)} \quad 1$$

Here, F is the applied force (N), A is the sample area (m^2), and Δh is the difference in height (m) under compression from h, the initial height (m) of the sample.

2.6. Batch-mode testing

Equilibration testing was performed in batch mode at room temperature (25 °C). Clevasol® particles or slices of Clevasol®-PVACC were placed in glass vials containing 18.2 MΩ cm^{-1} Milli-Q H_2O (pH 7) or SGS (pH 7.1). These were then spiked with $^{137}Cs^{+}$ or $^{85}Sr^{2+}$ (used as a γ-emitting surrogate for the environmentally relevant $^{90}Sr^{2+}$, for ease of analysis as ^{90}Sr is a pure β^--emitter) and equilibrated on a mixing table for various time periods for the determination of the partition coefficient (k_d, mL/g) as per Eq. (2).

$$k_d = \frac{m_{Aq}.A_S}{A_{Aq}.m_S} \quad 2$$

Here, A_S is the activity (Bq) adhered to the sorbent particles; A_{Aq} is the activity (Bq) of the aqueous phase filtered from the particles; m_{Aq} is the total mass (g) of the aqueous phase and m_S is the sorbent mass (g).

To determine the uptake capacity (q_{max}, mg/g), solutions with varied concentrations of stable CsCl or $SrCl_2$ were equilibrated on a mixing table for 48 h to ensure sorbent equilibration; stable Cs and Sr salts were used for this testing to avoid having to work with large radioactivities. The aqueous phase in all experiments was separated using a 0.45 μm borosilicate syringe filter and prepared for counting by HPGe γ-spectrometry, ICP-OES or ICP-QQQ as appropriate.

m_S for experiments with Clevasol®-PVACC slices refers to the mass of the Clevasol® resin within the slice and not the mass of the functionalised cryogel; this was estimated according to the saturated mass of the slice and by assuming a homogenous particle distribution throughout the material. k_d values are defined by the system having reached sorbent equilibrium. The time-integrated k_d, calculated in the same manner using Eq. (2) but prior to the system being sorbent equilibrium, is defined herein as $k_{t(x)}$ with the equilibration period (in batch mode) specified as x minutes. Combined method uncertainties were calculated with coverage factor (k) = 2, as per Section II of the SI. The cation-exchange efficiency (CEC) at equilibrium was calculated by Eq (3):

$$CEC\ [\%] = \left[\frac{(A_0 - A_e)}{A_0}\right] x100 \quad 3$$

where A_0 and A_e are the initial and equilibrium aqueous phase activities respectively.

2.7. Isotherm modelling

Uptake testing data were fitted to linearised Langmuir, Freundlich, Dubinin-Radushkevich and Temkin isotherm models to determine the mode of sorption.

2.7.1. Linear Langmuir isotherm model

The linear expression of the Langmuir isotherm model is outlined by Eq. (4).

$$\frac{c_e}{q_e} = \frac{1}{K_L\, q_{max}} + \frac{c_e}{q_{max}} \quad 4$$

$\frac{c_e}{q_e}$ *versus* c_e was plotted, whereby c_e is the equilibrium concentration of adsorbate on the Clevasol®; q_e is the ratio of Cs or Sr adsorbed per mass of the sorbent at equilibrium (mg/g); K_L is a constant related to the sorption capacity (mg/g); and q_{max} is the maximum sorption capacity (mg/g). The gradient and y-intercept of the linear graphs are used to calculate the unknowns.

2.7.2. Linear Freundlich isotherm model

The linear Freundlich isotherm model is expressed by Eq. (5), where parameters K_F and n are constants calculated from a plot of $\ln(q_e)$ *versus* $\ln(c_e)$.

$$\log(q_e) = \log(K_F) + \frac{1}{n}\log(c_e) \quad 5$$

2.7.3. Linear Dubinin-Radushkevich isotherm model

The linear Dubinin-Radushkevich isotherm model is expressed by Eq. (6), introducing the activity coefficient β ($mol^2.\ kJ^{-2}$) and the Polanyi potential ε (kJ/mol).

$$\ln(q_e) = \ln(q_{max}) - \beta.\varepsilon^2 \quad 6$$

ε is derived from Eq. (7).

$$\varepsilon = RT\ ln\left(1 + \frac{1}{c_e}\right) \quad 7$$

Here, R is the universal gas constant (8.314 J mol^{-1}/K) and T is the absolute temperature in Kelvin, K, where the experiments were performed at room temperature (298.15 K). $\ln(q_e)$ was plotted *versus* ε^2. The mean free energy of sorption, E (kJ/mol), can be determined using the β parameter of the Dubinin-Radushkevich isotherm, using Eq. (8).

$$E = 1\Big/\sqrt{2\beta} \quad 8$$

E is used to best indicate the sorption type. $E < 8$ kJ/mol would denote physisorption of the Cs or Sr onto the Clevasol; 8 kJ/mol $< E <$ 16 kJ/mol would indicate the prevalence of ion-exchange, whilst a much higher $E >$ 40 kJ/mol would reflect chemisorption [55,56].

2.7.4. Linear Temkin isotherm model

The linear Temkin isotherm model is expressed by Eq. (9).

$$q_e = B\ ln(A) + B\ ln(c_e) \quad 9$$

Here, B (J mol^{-1}) is a heat-of-sorption constant related via Eq. (10) to the Temkin constant b, which is related to the sorption energy. A (L.mg^{-1}) is the equilibrium binding constant.

$$B = \left(\frac{RT}{b}\right) \quad 10$$

$\ln(c_e)$ *versus* q_e was plotted to obtain the Temkin parameters.

2.8. Throughflow testing

Column experiments were performed to determine breakthrough curves for Cs and Sr in a simulated *in-situ* scenario, whereby contaminated groundwater would flow through the Clevasol®-PVACC in one direction. A closed system was assembled as per Fig. SI IV in the Supporting Information, whereby a Gilson Minipuls 3 peristaltic pump set to 0.09 rpm delivered the stable Cs or Sr influent solution constantly at 1.60–1.65 cm^3/h through the column. This flow is within the range of the Quaternary Upper aquifer at Sellafield [57]. Samples were collected at the base of the column throughout the experiment by a modified Redirac LKB 2112 fraction collector. The column (7 mm diameter x 58 mm length) was wet packed with Fisher Chemicals Extra Pure sand. System flow was visually verified using Bromocresol green, and the absence of Cs and Sr sorption onto the sand was confirmed by passing influent through the column when only packed with sand. The experiment was then run with a 1 mm layer of Clevasol®, of mass between 37.4 and 39.6 mg, at the base below the sand. Influent solutions contained stable Sr or Cs at a concentration of 20 ppm, made by dissolving CsCl or $SrCl_2 \cdot 6H_2O$ in Milli-Q H_2O or SGS. Sr samples were measured using a Thermo Scientific CAP 6000 series ICP-OES. Cs samples were measured with an Agilent 8800 Triple Quad ICP-MS, with samples diluted in 2.5% HNO_3 with a 5 ppb internal Re standard and using a peristaltic pump at 1 mL/min.

2.9. Desorption testing

Following loading with ^{137}Cs and ^{85}Sr during batch equilibration tests, Clevasol®-PVACC slices were leached in 10 ml 0.1 M HCl and agitated on a mixing table for 72 h. This was performed to simulate the response of the material to mild acidity in the environment which could readily occur in scenarios such as chemical leaks and acid rain infiltration. Aliquots of the filtrate were then extracted and prepared for HPGe γ-spectrometry to quantify recovery of adsorbed ^{137}Cs or ^{85}Sr back into the aqueous phase.

3. Results and discussion

3.1. Material characterisation

Clevasol®-PVACC's structure displays the intended interconnected microporous structure following its synthesis (Fig. SI V of the Supporting Information). A tentatively identified embedded Clevasol® particle appears partially coated by the cryogel polymer.

The incorporation of Clevasol® particles in the Clevasol®-PVACC significantly reduces SSA relative to blank PVA-based cryogel without particles (Table 1). Using the reported materials and methodology herein, we found the blank PVA-based cryogel to have a significantly higher SSA than previously reported (~130 vs ~60 m^2/g [53]); we attribute this most probably to variations in molecular weight and deacetylation levels between PVA brands [58]. Previously, we reported cryogels based on CHI-polyelectrolyte complexes which also possess an internal mesoporous structure [59]; SSA of the cryogels presented in Table 1 are comparable to CHI-based functionalised cryogels based on CHI-GA with Pd or Au nanoparticles [50,52]. Clevasol®-PVACC had a higher Young's modulus (Table 1) and demonstrated better resistance to strain (Fig. SI VI in the Supporting Information) than the blank PVA cryogel, demonstrating that the incorporation of the Clevasol® particles into the PVA-based cryogel significantly increased the durability of the material. This is a beneficial trait for practical environmental application within PRBs. Functionalising a PVA-based cryogel with other fine-grained sorbent particles could possibly therefore also potentially enhance the structural integrity of the composite material relative to the blank material, which is promising for future research using PVA-based cryogels as a host matrix. Our additional testing to investigate the potential of CHI as an alternative polymer to PVA showed that the blank CHI-based cryogel had a higher rigidity than the PVA-based cryogel (*i.e.* undergoing lower strain at higher stresses, Fig. SI VI in the Supporting Information), indicating that it likely has a much higher resistance to hydrostatic pressure. However, this could equally indicate that CHI-based cryogels may be more brittle than PVA-based cryogels. Further research could therefore focus on the optimisation of the synthesis of cryogel-sorbent composites, including exploring the effects of particle incorporation into CHI-based cryogels.

Table 1
SSA and Young's modulus for blank (non-Clevasol®-loaded) cryogels (PVA-based and CHI-based) versus Clevasol®-PVACC.

Cryogel composition (% wt)	SSA ($m^2.g^{-1}$)	Young's Modulus (E_Y, kPa)
PVA 5%/GA 0.25%	131.730	34.0 ± 3.3
CHI 1% GA 0.25%	7.720	543 ± 54
PVA 5%/GA 0.25%/Clevasol® 10%	32.898	55.4 ± 17.6

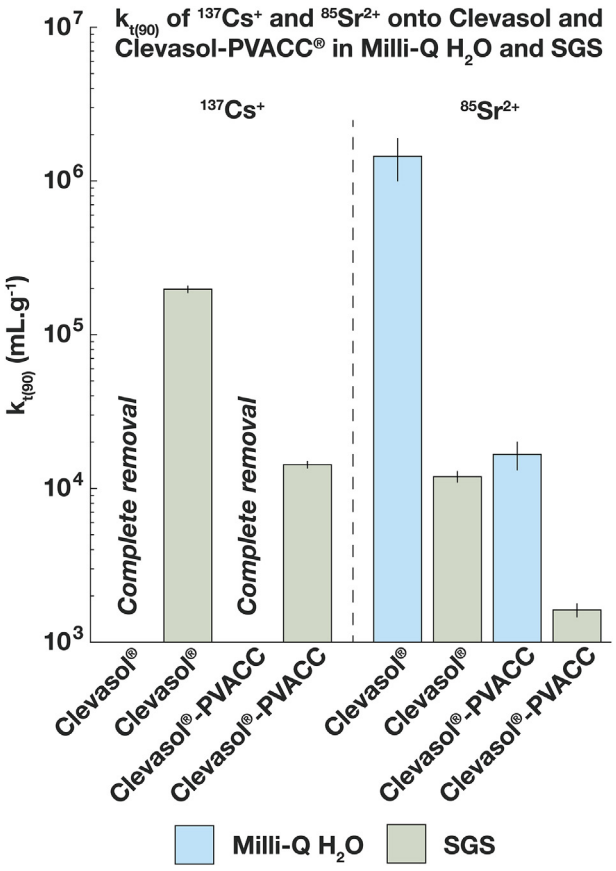

Fig. 1. of Clevasol® particles and Clevasol®-PVACC for $^{137}Cs^{+}$ and $^{85}Sr^{2+}$ in Milli-Q H_2O and SGS. Complete removal reflects that the activity in the aqueous phase was below the limit of detection.

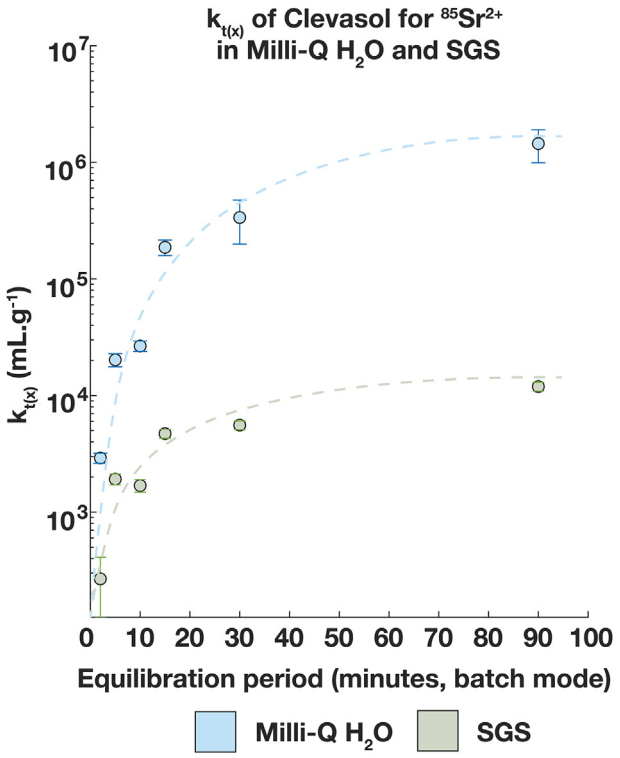

Fig. 2. Sorption kinetics ($k_{t(x)}$) of Clevasol® particles for $^{85}Sr^{2+}$ in Milli-Q H_2O and SGS.

3.2. Batch testing

The CEC of the non-bound Clevasol® resin particles in Milli-Q H_2O was 99.98% for $^{137}Cs^{+}$ and 99.80% for $^{85}Sr^{2+}$. The corresponding k_d were respectively 3.3 x 10^7 mL/g and 2.1 x 10^7 mL/g, demonstrating Clevasol® has an excellent affinity for both cations. This is amongst the highest k_d reported in the literature (see values reported in review articles highlighted in introduction section 1.2). The uptake kinetics and capacity were also excellent in SGS, with the $k_{t(90)}$ (effective k_d in SGS after 90 min of equilibration) of the non-bound Clevasol® particles at 2.0 x 10^5 mL/g for $^{137}Cs^{+}$ and 1.2 x 10^4 mL/g for $^{85}Sr^{2+}$ (Fig. 1 and Fig. 2). k_d values are often presented in associated literature to provide normalised values for the affinity of a sorbent material for its target contaminants, with effective k_d of $\geq 10^3$–10^4 mL/g generally being considered excellent [60,61]. The high $k_{t(90)}$ of Clevasol® for Cs and Sr demonstrate its rapid sorption kinetics (Fig. 1), whilst the effective k_d values at sorbent equilibrium in SGS would most probably be higher still if considering that the system was most likely not at equilibrium after 90 min. This is a critical trait for the intended deployment of our material in PRBs, where groundwater requires rapid decontamination during its passage through a material such as Clevasol®-PVACC.

$k_{t(90)}$ of Clevasol®-PVACC slices were also calculated in batch mode as 1.4 x 10^4 for $^{137}Cs^{+}$ and 1.6 x 10^3 for $^{85}Sr^{2+}$ in SGS (Fig. 1). The lower $k_{t(90)}$ of Clevasol®-PVACC compared to $k_{t(90)}$ of the non-cryogel-bound Clevasol® particles is logical, representing the time taken for diffusion of the radionuclides through the polymer walls of the cryogel to the bound Clevasol® particles. Further unpublished results from our lab incorporating a metal-organic framework into a PVA-based cryogel have shown that k_d of the sorbent material and the sorbent material bound within the cryogel is equal after 24 h. This shows that the uptake capacity of the resin was not hindered by its inclusion within our PVA-based cryogel, despite a slightly reduced rate of uptake.

We also note, based on elemental mapping, an even distribution of Cs and Sr adsorbed onto loaded Clevasol® particles which follows the particle topography (Fig. 3).

3.3. Isotherm parameters

Having established that Clevasol® and Clevasol®-PVACC have an excellent affinity for Cs^{+} and Sr^{2+}, we then investigated the sorption mechanism. Langmuir, Freundlich, Dubinin-Radushkevich and Temkin parameters from our testing are shown in Table 2. Cs^{+} and Sr^{2+} both demonstrated the closest fit in every case ($R^2 > 0.97$) to the Langmuir isotherm model in both Milli-Q H_2O and SGS, indicating monolayer coverage of Cs^{+} and Sr^{2+} adsorbed onto Clevasol® particles. The Langmuir uptake capacity (q_{max}) of Clevasol® for Cs^{+} and Sr^{2+} is competitive with other top-performing sorbents (see review articles mentioned in introduction Section 1.2), even when q_{max} is reduced in SGS for both elements relative to in Milli-Q H_2O. This effect is expected, as SGS contains spectator ions (*e.g.* Mg^{2+}, Ca^{2+} etc.). This nonetheless demonstrates a high effectiveness of Clevasol® for Cs^{+} and Sr^{2+} removal from the more complex SGS solution. The values obtained for the mean free energy of sorption (E) obtained through applying the Dubinin-Radushkevich isotherm (Table 2) in every case indicated that chemisorption was the sorption type of the Cs^{+} and Sr^{2+} onto the Clevasol® in each the Milli-Q H_2O and SGS solutions [55,56]. The positive B values obtained through applying the Temkin isotherm indicate that the adsorption process is exothermic.

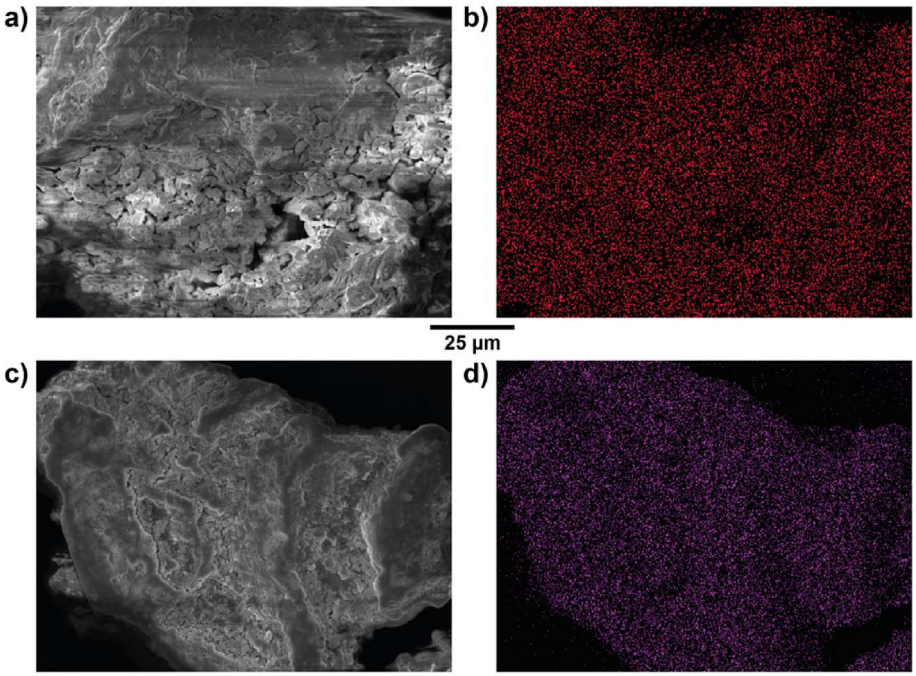

Fig. 3. a) SEM photomicrograph of Cs-loaded Clevasol® particle. b) Elemental mapping of Cs-distribution across the particle shown in a). c) SEM photomicrograph of Sr-loaded Clevasol® particle. d) Elemental mapping of Sr-distribution across the particle shown in c).

3.4. Desorption testing

We examined the retention of Cs and Sr within Clevasol®-PVACC, to detect how easily they may be desorbed under certain conditions once bound. To simulate the contamination of a Clevasol®-PVACC PRB with an acidic plume, which is a possibility at nuclear sites (*e.g.* Hanford site tank leaks can produce extremes of pH [62]), we immersed slices of radionuclide-loaded Clevasol®-PVACC (which had been loaded with ^{137}Cs and ^{85}Sr during batch testing) in 0.1 M HCl on a mixing table for 3 days. Here, we detected no ^{137}Cs in the leachate from the Clevasol®-PVACC, however 2–3% of the ^{85}Sr activity was recovered (relative to the activity $A_S A_S$ calculated to have been captured on the material during the relevant batch uptake experiment). We attribute this to a small degree of ^{85}Sr leaching from the Clevasol® resin, or perhaps non-bound ^{85}Sr residing in either the polymer structure or any solution remaining in the cryogel pores following filtration. Overall, the fact we detected no ^{137}Cs and a very small quantity of ^{85}Sr after this time demonstrates that Clevasol®-PVACC strongly retains both FPs at pH 1, which we consider in any case should be beyond the range of groundwater plumes acidified from on-site tank leaks.

3.5. Throughflow testing

Fig. 4 demonstrates that Cs^+ is more strongly bound to the Clevasol® resin than Sr^{2+}, as Cs^+ was only detected once ~40 g of effluent had passed through the column, compared to ~10 g for Sr^{2+} in Milli-Q and 20 g in SGS (Fig. 4). These data are consistent with the higher k_d of Clevasol® for Cs^+ than for Sr^{2+}, in addition to the acid leaching desorption tests where Cs^+ was not detected in the effluent. Secondly, the breakthrough for Sr^{2+} in Milli-Q water is faster than that for SGS, which is an unexpected result given that our other data demonstrates Clevasol® has a higher affinity for Sr in Milli-Q water (Figs. 1 and 2). Although we cannot objectively identify the reason for this, we rule out pH changes between the Milli-Q water (pH = 7.0) and SGS (pH = 7.1) as only minor quantities of Sr^{2+} were detected in leachates from the acid leaching test.

3.6. Considerations for practical deployment

To examine the potential use of a Clevasol®-PVACC PRB at scale, several factors must be considered to advance from the laboratory- to pilot-scale. Firstly, a scalable synthesis is required to produce adequate amounts of Clevasol®-PVACC for PRBs at the multi-kg

Table 2
Uptake capacity testing data fit to Langmuir, Freundlich, Dubinin-Radushkevich and Temkin isotherm parameters.

Analyte	Host Solution	K_L (mL/g)	Langmuir Parameters		Freundlich Parameters			
			q_{max} (mg/g)	R^2	K_F (mL/g)	1/n	n	R^2
Cs^+	Milli-Q	3.05×10^4	520	0.9762	2.54×10^{-4}	0.511	1.956	0.6674
	SGS	4.10×10^4	298	0.9932	2.10×10^{-1}	0.495	2.021	0.7825
Sr^{2+}	Milli-Q	1.80×10^5	145	0.9992	2.58×10^{-2}	0.377	2.650	0.6738
	SGS	5.13×10^4	128	0.9919	3.55×10^{-2}	0.491	2.037	0.8558

Analyte	Host Solution	q_{max}	Dubinin-Radushkevich Parameters			Temkin Parameters		
			β	***E***	R^2	***A***	***B***	R^2
Cs^+	Milli-Q	533	1.91×10^{-6}	512	0.8746	1.38	81.3	0.9412
	SGS	123	1.50×10^{-5}	183	0.6564	0.88	418	0.8506
Sr^{2+}	Milli-Q	124	5.72×10^{-7}	1322	0.9860	9.01	16.5	0.8478
	SGS	47	1.23×10^{-6}	638	0.7020	4.25×10^{-4}	20.5	0.9384

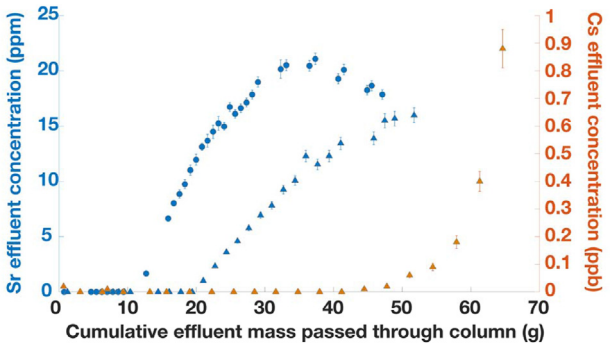

Fig. 4. Breakthrough curves of Cs^{+} and Sr^{2+} through Clevasol®-loaded sand columns. Blue represents Sr (left y-axis), orange represents Cs (right y-axis). Circles represent Milli-Q water as the aqueous phase, triangles represent SGS as the aqueous phase. No Cs data in Milli-Q presented as no Cs was detected in the column effluent, indicating essentially complete removal in the column.

scale. PVA and glutaraldehyde are both readily available commercial products which are made on industrial scales and relatively cheap. Although scaling up the manufacture of a material can lead to a reduction in the quality of its essential characteristics (*e.g.* in the case of functionalised cryogels, the pore size and particle distribution), recent work on scalable functionalised cryogels reported by Busquets et al. [51] demonstrated the expected uniform pore sizes and particle distributions. In their systems, material properties were easily controlled and were reported to be homogeneous at scales $\geq$400 mL, with multi-kg quantities being easily synthesised within several days [51].

A significant advantage that the Clevasol® resin itself has over other inorganic ion-exchange resins is that it is vitrifiable. Once a Clevasol®-PVACC PRB has reached the end of its life cycle, the resin could therefore be extracted and vitrified if it has captured significant activities. This is a desirable trait for long-term storage or disposal in geological nuclear waste repositories if large activities are captured at a contaminated site, to ensure that otherwise mobile radionuclides remain immobile in the repository. There also remains scope to explore the possibility that Clevasol®-PVACC could be reused after regeneration by stronger acid treatment, as has been demonstrated successfully with other functionalised cryogels for heavy metal capture [49,63]. This raises the prospect that systems such as Clevasol®-PVACC could possibly be installed on site and recycled as appropriate with periodic acid washing. Vitrification and the potential to explore the capability of the material for reuse demonstrate that there is a clear disposal path and a potential recycling path for the radionuclide-loaded material following its deployment, which has clear 'green chemistry'/sustainability benefits.

4. Conclusion

We have demonstrated that Clevasol® resin particles can be embedded into a PVA-based cryogel, producing a cheap composite material (Clevasol®-PVACC) with a facile and replicable synthesis. Our data demonstrates that Clevasol® resin particles have exceptionally high k_d for Cs^{+} and Sr^{2+}, whilst the composite material Clevasol®-PVACC is also highly effective for the removal of Cs^{+} and Sr^{2+} under the groundwater conditions at the Sellafield nuclear site, demonstrating a strong potential for effective *in-situ* application. There remains additional potential to explore the recyclability of Clevasol and Clevasol®-PVACC, by testing the ability of both Clevasol and Clevasol®-PVACC to be regenerated for future application after elution of the adsorbed radionuclides. Additionally, exploring the selectivity of Clevasol and Clevasol®-PVACC for Cs^{+} and Sr^{2+} in different concentrations of various other spectator ions could also provide an assessment of the capabilities of the materials to be employed in other environments, including for example in seawater and spent fuel storage pools. We consider that the scaled-up field application of Clevasol®-PVACC in PRB format would likely be most effective if employed in combination with engineered impermeable barriers, such as concrete or frozen ground, to direct the groundwater flow from a larger area into a smaller channel through the PRB. Overall, we believe we have shown that Clevasol®-PVACC shows excellent potential to be implemented as an interceptive PRB, which could be installed in the case of a fission product leak, or as an additional lasting 'failsafe' in combination with other direct and targeted remediation methods (*e.g.* groundwater pumping and treatment, electrokinetics) for groundwater plumes contaminated with ^{137}Cs and ^{90}Sr.

Credit author statement

Joshua D Chaplin: Conceptualisation, Methodology, Software, Validation, Formal analysis, Investigation, Data Curation, Writing-Original Draft, Writing- Review & Editing, Visualisation, Project administration.

Dmitriy Berillo: Conceptualisation, Methodology, Validation, Formal analysis, Investigation, Resources, Writing- Review & Editing, Funding acquisition.

Jamie Purkis: Formal analysis, Investigation; Resources, Methodology, Validation, Writing - Review & Editing.

Marie L. Byrne: Formal analysis, Investigation, Writing - Review & Editing.

Alexandre D.C·C.M Tribolet: Investigation; Writing - Review & Editing.

Phillip E. Warwick: Conceptualisation, Funding acquisition, Methodology; Project administration; Resources, Supervision, Writing - Review & Editing.

Andrew B. Cundy: Conceptualisation, Funding acquisition, Methodology; Project administration; Resources, Supervision, Writing - Review & Editing.

Funding sources

Laboratory materials were supplied by GAU-Radioanalytical (National Oceanography Centre, University of Southampton) and the School of Pharmacy and biomolecular Science (University of Brighton).

Declaration of competing interest

The authors declare that they have no known competing financial interests or personal relationships that could have appeared to influence the work reported in this paper.

Acknowledgment

We thank ADePhine GmbH (Bern, Switzerland) for supplying the Clevasol® resin for our testing. D Berillo acknowledges the European Union's Horizon 2020 Research and Innovation Programme (under the Marie Skłodowska-Curie Fellowship grant agreement 701289) which supported time when writing this paper. A B Cundy, P E Warwick and J M Purkis acknowledge funding from the TRANSCEND (TRANsformative SCience and Engineering for Nuclear Decommissioning) consortium (EPSRC grant number EP/S01019X/1). We thank three peer reviewers for improving the manuscript through their comments.

Appendix A. Supplementary data

Supplementary data to this article can be found online at https://doi.org/10.1016/j.mtsust.2022.100190.

References

[1] P. Reeve, K. Eilbeck, Contaminated land and groundwater management at Sellafield, a large operational site with significant legacy and contaminated land challenges, in: Proc. ICEM2007 - 11th Int. Conf. Environ. Remediat. Radioact. Waste Manag, 2007, https://doi.org/10.1115/ICEM2007-7051.

[2] J. Cruickshank, Findings of the Sellafield Contaminated Land & Groundwater Management Project and the Next Steps for the Land Quality Programme, 2012.

[3] G.L. Edgemon, V.S. Anda, H.S. Berman, M.E. Johnson, K.D. Boomer, History and operation of the hanford high-level waste storage tanks, Corrosion 65 (2009) 163–174, https://doi.org/10.5006/1.3319125.

[4] M. Castrillejo, N. Casacuberta, C.F. Breier, S.M. Pike, P. Masqué, K.O. Buesseler, Reassessment of 90Sr, 137Cs, and 134Cs in the coast off Japan derived from the fukushima dai-ichi nuclear accident, Environ. Sci. Technol. 50 (2016) 173–180, https://doi.org/10.1021/acs.est.5b03903.

[5] K. Taniguchi, Y. Onda, H.G. Smith, W. Blake, K. Yoshimura, Y. Yamashiki, T. Kuramoto, K. Saito, Transport and redistribution of radiocesium in fukushima fallout through rivers, Environ. Sci. Technol. 53 (2019) 12339–12347, https://doi.org/10.1021/acs.est.9b02890.

[6] K. Buesseler, M. Dai, M. Aoyama, C. Benitez-Nelson, S. Charmasson, K. Higley, V. Maderich, P. Masqué, P.J. Morris, D. Oughton, J.N. Smith, Fukushima daiichi–derived radionuclides in the ocean: transport, fate, and impacts, Ann. Rev. Mar. Sci 9 (2017) 173–203, https://doi.org/10.1146/annurev-marine-010816-060733.

[7] V. Kenyon, J.A. Buesseler, K.O. Casacuberta, N. Castrillejo, M. Otosaka, S. Masqué, P. Drysdale, J.A. Pike, S.M. Sanial, J.A. Kenyon, K.O. Buesseler, N. Casacuberta, M. Castrillejo, S. Otosaka, P. Masqué, J.A. Drysdale, S.M. Pike, V. Sanial, Distribution and evolution of fukushima dai-ichi derived 137Cs, 90Sr, and 129I in surface seawater off the coast of Japan, Environ. Sci. Technol. 54 (2020) 15066–15075, https://doi.org/10.1021/acs.est.0c05321.

[8] J.M. Purkis, P.E. Warwick, J. Graham, S.D. Hemming, A.B. Cundy, Towards the application of electrokinetic remediation for nuclear site decommissioning, J. Hazard Mater. 413 (2021) 125274, https://doi.org/10.1016/j.jhazmat.2021.125274.

[9] International Atomic Energy Agency, Energy, Electricity and Nuclear Power Estimates for the Period up to 2050, 2020. Vienna, https://www.iaea.org/publications/14786/energy-electricity-and-nuclear-power-estimates-for-the-period-up-to-2050.

[10] S. Yu, H. Tang, D. Zhang, S. Wang, M. Qiu, G. Song, D. Fu, B. Hu, X. Wang, MXenes as emerging nanomaterials in water purification and environmental remediation, Sci. Total Environ. 811 (2022), https://doi.org/10.1016/j.scitotenv.2021.152280.

[11] X. Liu, H. Pang, X. Liu, Q. Li, N. Zhang, L. Mao, M. Qiu, B. Hu, H. Yang, X. Wang, Orderly porous covalent organic frameworks-based materials: superior adsorbents for pollutants removal from aqueous solutions, Innov 2 (2021), https://doi.org/10.1016/j.xinn.2021.100076.

[12] D. Li, D.I. Kaplan, A.S. Knox, K.P. Crapse, D.P. Diprete, Aqueous 99Tc, 129I and 137Cs removal from contaminated groundwater and sediments using highly effective low-cost sorbents, J. Environ. Radioact. 136 (2014) 56–63, https://doi.org/10.1016/j.jenvrad.2014.05.010.

[13] T. Missana, M. Garcia-Gutierrez, U. Alonso, Sorption of strontium onto illite/smectite mixed clays, Phys. Chem. Earth 33 (2008) S156–S162, https://doi.org/10.1016/j.pce.2008.10.020.

[14] E.H. Borai, R. Harjula, L. malinen, A. Paajanen, Efficient removal of cesium from low-level radioactive liquid waste using natural and impregnated zeolite minerals, J. Hazard Mater. 172 (2009) 416–422, https://doi.org/10.1016/j.jhazmat.2009.07.033.

[15] P. Sylvester, A. Clearfield, The removal of strontium and cesium from simulated hanford groundwater using inorganic ion exchange materials, Solvent Extr. Ion Exch. 16 (1998) 1527–1539, https://doi.org/10.1080/07366299808934593.

[16] P.A. Taylor, Development of a Passive-Flow Treatment System for {sup 90}Sr-Contaminated Seep Water at Waste Area Grouping 5 at Oak Ridge National Laboratory, 1994, https://doi.org/10.2172/10104666. Oak Ridge, TN.

[17] S.M. Seneca, A.J. Rabideau, Natural zeolite permeable treatment wall for removing Sr-90 from groundwater, Environ. Sci. Technol. (2013), 130117145422000, https://doi.org/10.1021/es304008r.

[18] P.G. Heath, M.W.A. Stewart, S. Moricca, N.C. Hyatt, Hot-isostatically pressed wasteforms for Magnox sludge immobilisation, J. Nucl. Mater. 499 (2018) 233–241, https://doi.org/10.1016/J.JNUCMAT.2017.11.034.

[19] B. Pangeni, H. Paudyal, K. Inoue, H. Kawakita, K. Ohto, M. Gurung, S. Alam, Development of low cost adsorbents from agricultural waste biomass for the removal of Sr(II) and Cs(I) from water, Waste and Biomass Valorization 5 (2014) 1019–1028, https://doi.org/10.1007/s12649-014-9309-4.

[20] S.M. Yakout, E. Elsherif, Investigation of strontium (II) sorption kinetic and thermodynamic onto straw-derived biochar, Part, Sci. Technol. 33 (2015) 579–586, https://doi.org/10.1080/02726351.2015.1008712.

[21] S. Yamauchi, T. Yamagishi, K. Kirikoshi, M. Yatagai, Cesium adsorption from aqueous solutions onto Japanese oak charcoal I: effects of the presence of group 1 and 2 metal ions, J. Wood Sci. 60 (2014) 473–479, https://doi.org/10.1007/s10086-014-1431-1.

[22] A. Arifi, H.A. Hanafi, Adsorption of cesium, thallium, strontium and cobalt radionuclides using activated carbon, Asian J. Chem. 23 (2011) 111, https://doi.org/10.4208/jams.100809.112309a.

[23] R. Chiarizia, E.P. Horwitz, R.A. Beauvais, S.D. Alexandratos, DIPHONIX-CS : a novel combined cesium and strontium selective ION exchange resin, Solvent Extr. Ion Exch. 16 (1998) 875–898, https://doi.org/10.1080/07366299808934558.

[24] M.R. Duignan, C.A. Nash, Removal of cesium from savannah river site waste with spherical resorcinol formaldehyde ion exchange resin: experimental tests, Sep. Sci. Technol. 45 (2010) 1828–1840, https://doi.org/10.1080/01496395.2010.493105.

[25] A.S. Toropov, A.R. Satayeva, S. Mikhalovsky, A.B. Cundy, The use of composite ferrocyanide materials for treatment of high salinity liquid radioactive wastes rich in cesium isotopes, Radiochim. Acta 102 (2014) 911–917, https://doi.org/10.1515/ract-2013-2212.

[26] A.K. Vipin, S. Ling, B. Fugetsu, Sodium cobalt hexacyanoferrate encapsulated in alginate vesicle with CNT for both cesium and strontium removal, Carbohydr. Polym. 111 (2014) 477–484, https://doi.org/10.1016/J.CARBPOL.2014.04.037.

[27] D. Ding, Z. Zhang, R. Chen, T. Cai, Selective removal of cesium by ammonium molybdophosphate – polyacrylonitrile bead and membrane, J. Hazard Mater. 324 (2017) 753–761, https://doi.org/10.1016/J.JHAZMAT.2016.11.054.

[28] Y. Wu, C.P. Lee, H. Mimura, X. Zhang, Y. Wei, Stable solidification of silica-based ammonium molybdophosphate by allophane: application to treatment of radioactive cesium in secondary solid wastes generated from fukushima, J. Hazard Mater. 341 (2018) 46–54, https://doi.org/10.1016/j.jhazmat.2017.07.044.

[29] S.V. Ingale, R. Ram, P.U. Sastry, P.B. Wagh, R. Kumar, R. Niranjan, S.B. Phapale, R. Tewari, A. Dash, S.C. Gupta, Synthesis and characterization of ammonium molybdophosphate-silica nano-composite (AMP-SiO2) as a prospective sorbent for the separation of137Cs from nuclear waste, J. Radioanal. Nucl. Chem. 301 (2014) 409–415, https://doi.org/10.1007/s10967-014-3143-9.

[30] S. Yoshida, Y. Kimura, I. Ogino, S.R. Mukai, Synthesis of a microhoneycomb-type silica-supported ammonium molybdophosphate for cesium separation, J. Chem. Eng. Jpn. 46 (2013) 616–619, https://doi.org/10.1252/jcej.13we064.

[31] A. Mudhoo, D. Mohan, C.U. Pittman, G. Sharma, M. Sillanpaa, Adsorbents for real-scale water remediation: gaps and the road forward, J. Environ. Chem. Eng. 9 (2021), https://doi.org/10.1016/j.jece.2021.105380.

[32] S. Chen, J. Hu, S. Han, Y. Guo, N. Belzile, T. Deng, A review on emerging composite materials for cesium adsorption and environmental remediation on the latest decade, Sep. Purif. Technol. 251 (2020), https://doi.org/10.1016/j.seppur.2020.117340.

[33] J. Wang, S. Zhuang, Cesium separation from radioactive waste by extraction and adsorption based on crown ethers and calixarenes, Nucl. Eng. Technol. 52 (2020), https://doi.org/10.1016/j.net.2019.08.001.

[34] J. Wang, S. Zhuang, Y. Liu, Metal hexacyanoferrates-based adsorbents for cesium removal, Coord. Chem. Rev. 374 (2018), https://doi.org/10.1016/j.ccr.2018.07.014.

[35] M. Jiménez-Reyes, P.T. Almazán-Sánchez, M. Solache-Ríos, Radioactive waste treatments by using zeolites. A short review, J. Environ. Radioact. 233 (2021), https://doi.org/10.1016/j.jenvrad.2021.106610.

[36] N. Koshy, P. Pathak, Removal of strontium by physicochemical adsorptions and ion exchange methods, Handb. Environ. Chem. 88 (2020) 185–202, https://doi.org/10.1007/978-3-030-15314-4_10.

[37] S. Yu, H. Pang, S. Huang, H. Tang, S. Wang, M. Qiu, Z. Chen, H. Yang, G. Song, D. Fu, B. Hu, X. Wang, Recent advances in metal-organic framework membranes for water treatment: a review, Sci. Total Environ. 800 (2021), https://doi.org/10.1016/j.scitotenv.2021.149662.

[38] H.F. Liu, T.W. Qian, D.Y. Zhao, Reductive immobilization of perrhenate in soil and groundwater using starch-stabilized ZVI nanoparticles, Chin. Sci. Bull. 58 (2013) 275–281, https://doi.org/10.1007/s11434-012-5425-3.

[39] C. Ding, W. Cheng, Y. Sun, X. Wang, Novel fungus-Fe_3O_4 bio-nanocomposites as high performance adsorbents for the removal of radionuclides, J. Hazard Mater. 295 (2015) 127–137, https://doi.org/10.1016/j.jhazmat.2015.04.032.

[40] J.D. Chaplin, P.E. Warwick, A.B. Cundy, F. Bochud, P. Froidevaux, Novel DGT configurations for the assessment of bioavailable plutonium, americium, and uranium in marine and freshwater environments, Anal. Chem. 93 (2021) 11937–11945, https://doi.org/10.1021/acs.analchem.1c01342.

[41] J.D. Chaplin, M. Christl, M. Straub, F. Bochud, P. Froidevaux, Passive sampling tool for actinides in spent nuclear fuel pools, ACS Omega 7 (2022) 20053–20058, https://doi.org/10.1021/acsomega.2c01884.

[42] N. Hammi, S. Chen, F. Dumeignil, S. Royer, A. El Kadib, Chitosan as a sustainable precursor for nitrogen-containing carbon nanomaterials: synthesis and uses, Mater. Today Sustain. 10 (2020), https://doi.org/10.1016/j.mtsust.2020.100053.

[43] K. Chullasat, P. Nurerk, P. Kanatharana, P. Kueseng, T. Sukchuay, O. Bunkoed, Hybrid monolith sorbent of polypyrrole-coated graphene oxide incorporated into a polyvinyl alcohol cryogel for extraction and enrichment of sulfonamides from water samples, Anal. Chim. Acta 961 (2017) 59–66, https://doi.org/10.1016/j.aca.2017.01.052.

[44] I.E. Veleshko, V.V. Nikonorov, A.N. Veleshko, E.V. Rumyantseva, S.N. Mikhailov, V.I. Lozinskii, R.V. Ivanov, L.S. Gal'braikh, N.R. Kil'deeva, Sorption of Eu(III)

from solutions of covalently cross-linked chitosan cryogels, Fibre Chem. 42 (2011) 364–369, https://doi.org/10.1007/s10692-011-9287-2.
[45] M.K. Modi, P. Pattanaik, N. Dash, S. Subramanian, Sorption of radionuclides, Int. J. Pharm. Sci. Rev. Res. 34 (2015) 122–130.
[46] J. Pospěchová, V. Brynych, V. Štengl, J. Tolasz, J.H. Langecker, M. Bubeníková, L. Szatmáry, Polysaccharide biopolymers modified with titanium or nickel nanoparticles for removal of radionuclides from aqueous solutions, J. Radioanal. Nucl. Chem. 307 (2016) 1303–1314, https://doi.org/10.1007/s10967-015-4414-9.
[47] I.N. Savina, C.J. English, R.L.D. Whitby, Y. Zheng, A. Leistner, S.V. Mikhalovsky, A.B. Cundy, High efficiency removal of dissolved As(III) using iron nanoparticle-embedded macroporous polymer composites, J. Hazard Mater. 192 (2011) 1002–1008, https://doi.org/10.1016/j.jhazmat.2011.06.003.
[48] I.N. Savina, G.C. Ingavle, A.B. Cundy, S.V. Mikhalovsky, A simple method for the production of large volume 3D macroporous hydrogels for advanced biotechnological, medical and environmental applications, Sci. Rep. 6 (2016) 1–9, https://doi.org/10.1038/srep21154.
[49] A.Z. Baimenov, D.A. Berillo, K. Moustakas, V.J. Inglezakis, Efficient removal of mercury (II) from water by use of cryogels and comparison to commercial adsorbents under environmentally relevant conditions, J. Hazard Mater. 399 (2020) 123056, https://doi.org/10.1016/j.jhazmat.2020.123056.
[50] D. Berillo, Gold nanoparticles incorporated into cryogel walls for efficient nitrophenol conversion, J. Clean. Prod. 247 (2020) 119089, https://doi.org/10.1016/j.jclepro.2019.119089.
[51] R. Busquets, A.E. Ivanov, L. Mbundi, S. Hörberg, O.P. Kozynchenko, P.J. Cragg, I. N. Savina, R.L.D. Whitby, S.V. Mikhalovsky, S.R. Tennison, H. Jungvid, A.B. Cundy, Carbon-cryogel hierarchical composites as effective and scalable filters for removal of trace organic pollutants from water, J. Environ. Manag. 182 (2016) 141–148, https://doi.org/10.1016/j.jenvman.2016.07.061.
[52] D. Berillo, A. Cundy, 3D-macroporous chitosan-based scaffolds with in situ formed Pd and Pt nanoparticles for nitrophenol reduction, Carbohydr. Polym. 192 (2018) 166–175, https://doi.org/10.1016/j.carbpol.2018.03.038.
[53] V.M. Gun'ko, I.N. Savina, S.V. Mikhalovsky, Cryogels: morphological, structural and adsorption characterisation, Adv. Colloid Interface Sci. 187–188 (2013) 1–46, https://doi.org/10.1016/J.CIS.2012.11.001.
[54] H. Kirsebom, L. Elowsson, D. Berillo, S. Cozzi, I. Inci, E. Piskin, I.Y. Galaev, B. Mattiasson, Enzyme-catalyzed crosslinking in a partly frozen state: a new way to produce supermacroporous protein structures, Macromol. Biosci. 13 (2013) 67–76, https://doi.org/10.1002/mabi.201200343.
[55] S. Vasiliu, I. Bunia, S. Racovita, V. Neagu, Adsorption of cefotaxime sodium salt on polymer coated ion exchange resin microparticles: kinetics, equilibrium and thermodynamic studies, Carbohydr. Polym. 85 (2011), https://doi.org/10.1016/j.carbpol.2011.02.039.
[56] S. Emik, Preparation and characterization of an IPN type chelating resin containing amino and carboxyl groups for removal of Cu(II) from aqueous solutions, React. Funct. Polym. 75 (2014), https://doi.org/10.1016/j.reactfunctpolym.2013.12.006.
[57] A.A. McMillan, J.A. Heathcote, B.A. Klinck, M.G. Shepley, C.P. Jackson, P.J. Degnan, Hydrogeological characterization of the onshore the concept of domains, Q. J. Eng. Geol. Hydrogeol. 33 (2000) 301–323.
[58] Y. Zheng, ACTIVATED CARBON & CARBON-CRYOGEL COMPOSITES FOR HAEMOPERFUSION BASED APPLICATIONS, University of Brighton, UK, 2013. http://eprints.brighton.ac.uk/12167/1/ACTIVATED CARBON %26 CARBON-CRYOGEL COMPOSITES FOR HAEMOPERFUSION BASED APPLICATIONS%28Yishan Zheng-June ~1.pdf. (Accessed 25 August 2018).
[59] D. Berillo, L. Elowsson, H. Kirsebom, Oxidized dextran as crosslinker for chitosan cryogel scaffolds and formation of polyelectrolyte complexes between chitosan and gelatin, Macromol. Biosci. 12 (2012) 1090–1099, https://doi.org/10.1002/mabi.201200023.
[60] M.J. Manos, N. Ding, M.G. Kanatzidis, Layered metal sulfides: exceptionally selective agents for radioactive strontium removal, Proc. Natl. Acad. Sci. USA 105 (2008) 3696–3699, https://doi.org/10.1073/pnas.0711528105.
[61] J. Lehto, A. Clearfield, The ion exchange of strontium on sodium titanate Na4Ti9O20.xH2O, J. Radioanal. Nucl. Chem. Lett. 118 (1987) 1–13, https://doi.org/10.1007/BF02165649.
[62] J.L. Krumhansl, K.L. Nagy, Phase Chemistry of Tank Sludge Residual Components, 2000. https://www.osti.gov/biblio/831171.
[63] S. Kudaibergenov, Z. Adilov, D. Berillo, G. Tatykhanova, Z. Sadakbaeva, K. Abdullin, I. Galaev, Novel macroporous amphoteric gels: preparation and characterization, Express Polym. Lett. 6 (2012) 346–353, https://doi.org/10.3144/expresspolymlett.2012.38.